Order and disorder in Durham polyacetylene

D. C. Bott, C. S. Brown, J. N. Winter and J. Barker
BP Research Centre, Chertsey Road, Sunbury-on-Thames, Middlesex TW16 7LN, UK
(Received 17 September 1986; accepted 30 October 1986)

The Durham route to polyacetylene provides, for the first time, the possibility of controlling the crystalline structure of this fascinating material. This control will enable us to probe the role of the redox doping and relative spatial co-ordinates of the chains in determining electrical conductivity. Before this can be accomplished it is necessary to understand the nature of the order within the variety of materials which can now be produced. Material produced from quiescent films can have a range of structures from largely amorphous (inasmuch as a structure composed of rigid rods can exhibit disorder) to slightly crystalline. By stretching the precursor film during transformation highly oriented, crystalline polyacetylene can be produced. This offers a range of structures and should enable the separation of inter- and intra-chain electronic effects for the first time.

(Keywords: Durham polyacetylene; precursor polymer; microstructure; crystallinity; band-tailing)

INTRODUCTION

'Polyacetylene is the simplest conducting polymer.' This statement, or something very close to it, is contained in the introductions of most reviews of conducting polymers. The author(s) then go on to describe the electrical conductivity, the nature of the charge carriers, or some other such property of the material concerned with its conductivity. They invariably forget the polymeric nature of the material. It was many years before anyone attempted to determine the molecular weight. Crystal structures are talked about as though the polymers were perfect crystals, instead of the disorganized, entangled messes that most polymer scientists would recognize. To some extent this is due to the intractability of polyacetylene produced by the conventional direct polymerization routes. Pragmatism has ruled and, since it could not be characterized or processed as a polymer, the consideration of its polymeric materials properties has been postponed. A breakthrough for polymer science came with the development of precursor routes to this fascinating group of materials. The Durham route to polyacetylene[1] was the first and still most widely reported of these, and will form the basis of this paper. Our intention is to start with molecular structure and end with the doping process and to examine each manifestation of disorder and its effect on the simple structure which people have taken as an *a priori* assumption. It is hoped that this strategy will convince the reader that, however fascinating the physics of these materials may be, it is boring when compared to the complexity of order present.

(1) MOLECULAR STRUCTURE

(1.1) Introduction

The great benefit of a precursor route is that the intermediate polymer is processible, enabling the production of the final product in the desired form. The polymer can also be purified by conventional reprecipitation techniques, and cast from solutions on a variety of substrates. Thus, the Durham precursor polymer (*Figure 1*) is soluble in solvents such as acetone and ethyl acetate, and can be purified and solution processed as a normal polymer.

The degree of order (or disorder) present in product polyacetylene will, to some extent, reflect that present in the precursor polymer. The precursor cast from solution is a randomly coiled amorphous polymer and it is most unlikely that a perfect crystalline polyacetylene could be obtained from it (*Figure 2*). What is not clear is the extent to which the precursor structure determines that of the product polyacetylene, bearing in mind possible structural relaxations brought about by the plasticizing effect of eliminated 1,2-bis(trifluoromethyl) benzene and the isomerization reaction. One of the few comparable systems is the dehydrochlorination of PVC to polyacetylene, but the relevant structural correlations are limited and inconclusive[2]. Some of the many available types of order and disorder possible in these complex systems are described in section (2.7.1) below.

The precursor polymer possesses two characteristics which may make a significant impact on attempts to obtain well ordered Durham polyacetylene.

The first derives from the considerable steric bulk of the precursor polymer's bicyclic side groups. Steric interactions will impose severe constraints upon the conformation of the polymer chain but the nature of these constraints will depend on the stereochemical microstructure. An attempt to understand these consequences of microstructure, using computer modelling, is described below. Unfortunately our ability to vary microstructure in reality is restricted by the need to use low temperatures and relatively reactive and unselective metathesis catalysts to assemble precursor polymers. This is not the case for non-eliminating analogues of the precursor[3] and examples of materials exhibiting a variety of microstructures have been made.

The second important characteristic stems from the thermal instability of the precursor, which means that the polymer is generally cast with varying short lengths of polyene sequences already present in the chain[4]. It is conceivable that such eliminated sequences may

0032-3861/87/040601-16$03.00
© 1987 Butterworth & Co. (Publishers) Ltd.

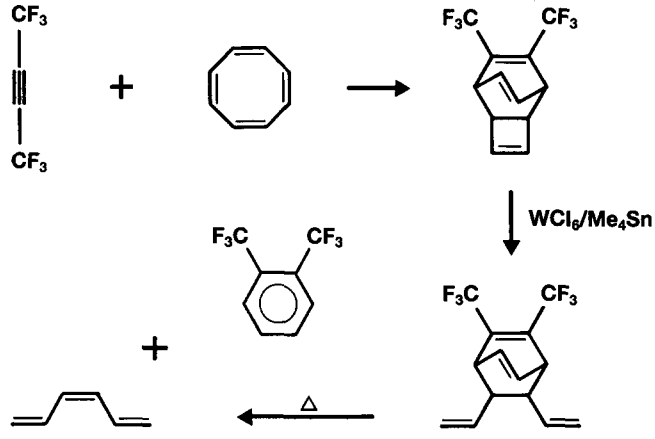

Figure 1 Durham route chemistry showing (a) formation of monomer, (b) polymerization step and (c) transformation

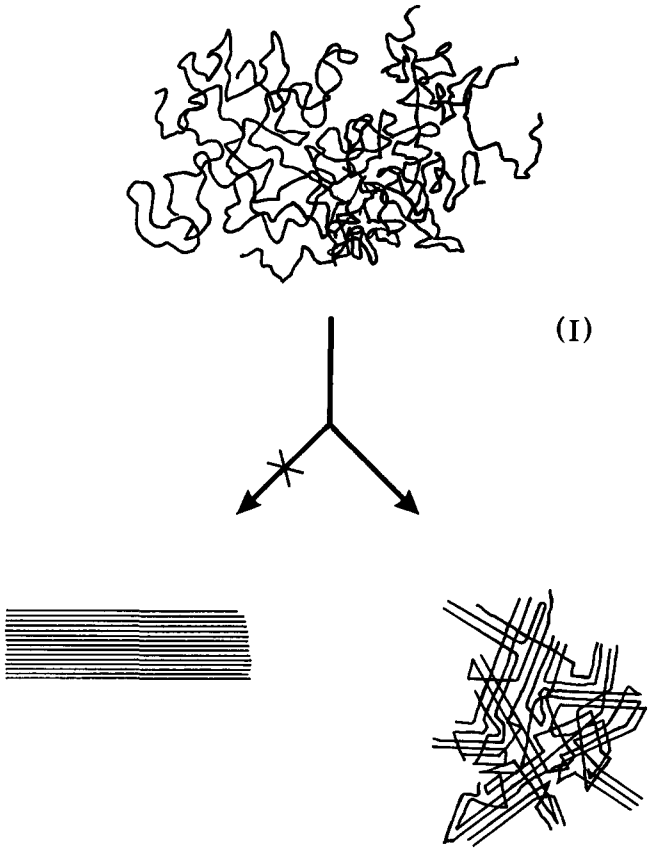

Figure 2 Random coil and possible transitions to perfect crystal (unlikely) and 'nematic' crystal

contribute to ordering in the precursor and they will certainly affect the above mentioned conformational constraints. However, the effect of polyenes will be dealt with only in passing and we will concentrate on the effect of pristine precursor polymer microstructure.

(1.2) The microstructure and conformation of the precursor polymer

The microstructure of metathesis polymers has been extensively reviewed[5] and the possible dyad structures have been described in detail[3]. Three of the four possible dyads are illustrated in *Figure 3* for the non-eliminating model system. The conformational consequences of assembling stereoregular Durham precursor polymers were investigated using the 'Chem Graf'[6] computer molecular modelling program. The non-eliminating model system was used in this study because some structural information was available for the crystal monomer[7].

The most stable conformation of assemblies of *trans* racemic (tr) dyads is a straight chain with the side groups taking up a pseudo-staggered relationship (*Figure 4*). There is little restriction on the rotation of the allylic bonds in the polymer backbone as the side groups are

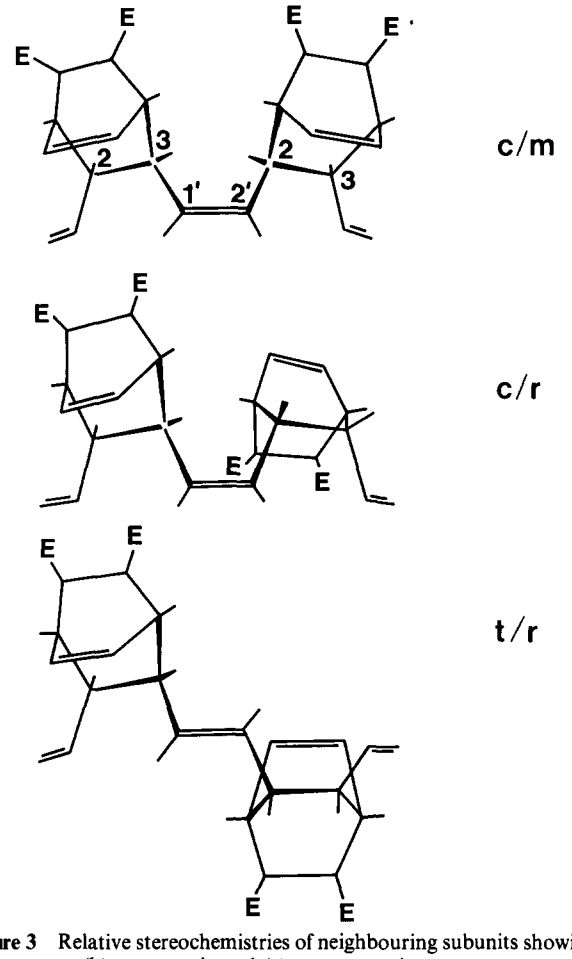

Figure 3 Relative stereochemistries of neighbouring subunits showing (a) *cis*-meso, (b) *cis*-racemic and (c) *trans*-racemic

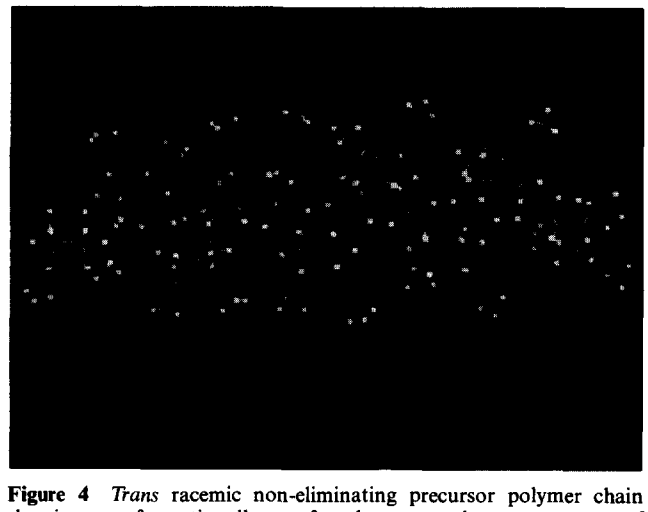

Figure 4 *Trans* racemic non-eliminating precursor polymer chain showing conformationally preferred staggered arrangement of sidegroups. This leads to a linear chain

held well away from each other by the *trans* double bond configuration and so an open random coil would reasonably be expected for a homo (tm) polymer. Similar conclusions can be drawn for the homo *trans* racemic (tr) assemblies.

The situation for homo *cis* assemblies is more interesting. The *cis* configuration holds the side groups quite close together and severely restricts the conformational possibilities for (cm) dyads (see *Figure 5*). Indeed, assembly of an homo (cm) polymer is not possible because rotation of the allylic bonds in the polymer backbone, sufficient to relieve the steric interactions in the dyad, sends the polymer chain crashing into itself after only a few monomer units (*Figure 6*). The constraints on (cr) dyads are less severe, but, to minimize steric interactions, homo (cr) polymers would be expected to prefer highly twisted helical conformations (*Figure 7*).

The precursor polymers are by no means stereoregular, but *cis* containing materials with only small *cis* blocks will be constrained to have tight bends in these regions and tightly coiled overall conformations. Unfortunately it is not possible at present, to test whether a high *trans* precursor would yield a more ordered polyacetylene than a high *cis* precursor, as an appropriate range of microstructures is not available.

It is more difficult to visualize the effect of eliminated sequences. The removal of the bulky side groups will relax local steric constraints, but the rigidity of the polyenes formed in place of mobile *trans* units may serve to accentuate conformational effects in remote *cis* precursor sequences (*Figure 8*).

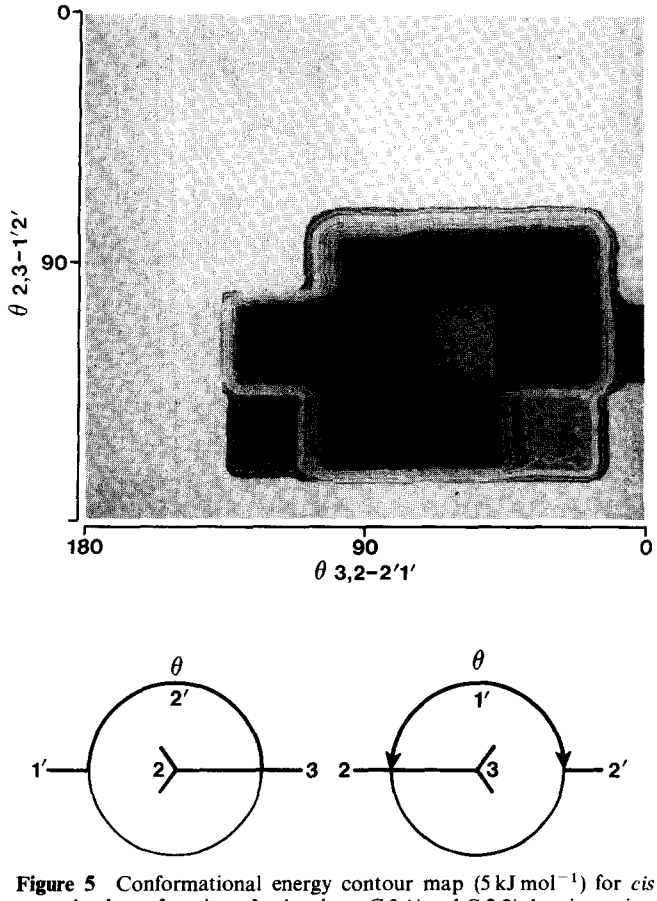

Figure 5 Conformational energy contour map (5 kJ mol^{-1}) for *cis* meso dyad as a function of twist about C 3,1′ and C 2,2′ showing twists necessary to relieve steric congestion of sidegroups (see *Figure 3* for numbering system)

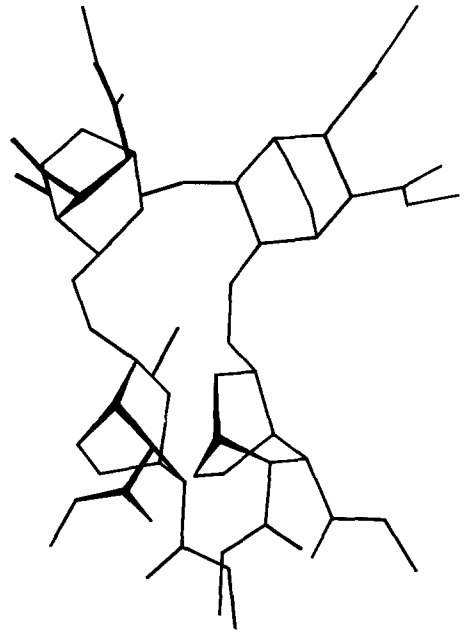

Figure 6 *Cis*-meso non-eliminating precursor polymer chain showing conformationally induced steric collision within 4 repeat units

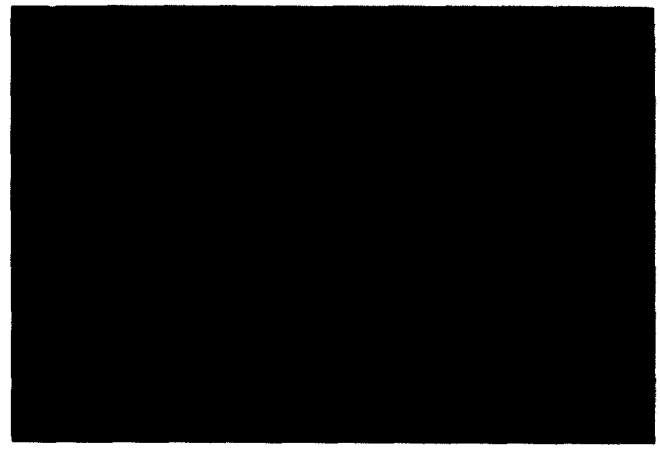

Figure 7 *Cis* racemic non-eliminating precursor polymer chain showing conformationally preferred helix

(*1.3*) *Carbon-13 n.m.r. of precursors and non-precursor analogues*

Once the theoretical considerations of microstructure are understood, it is necessary to probe the structures of the 'real' precursor polymers and monitor the effect of their structure on the order of the final product. The carbon-13 n.m.r. spectrum of the precursor polymer has been described elsewhere[3]. Since observed linewidths were very broad, and since the precursor cannot be prepared using stereoregulating catalysts, a microstructural analysis of the kind routinely applied to metathesis polymers of isomerically pure biaxially symmetric monomers[5] was not possible.

In the hope that the conclusions could be carried over to the precursor polymer, a carbon-13 n.m.r. study was made of a non-eliminating analogue (poly[[7,8-bis(carboxymethyl)bicyclo[2.2.2] octa-5-ene-2,3-diyl] 1,2-ethenediyl]) (**I**). The primary advantage of using this material is that the monomer 9,10-bis(carboxymethyl)tricyclo-[4.2.2.0^{2,5}]deca-3,7-diene (**II**) can be polymerized at higher temperatures by metathesis catalysts known to be stereoregulating in other systems. The structures of

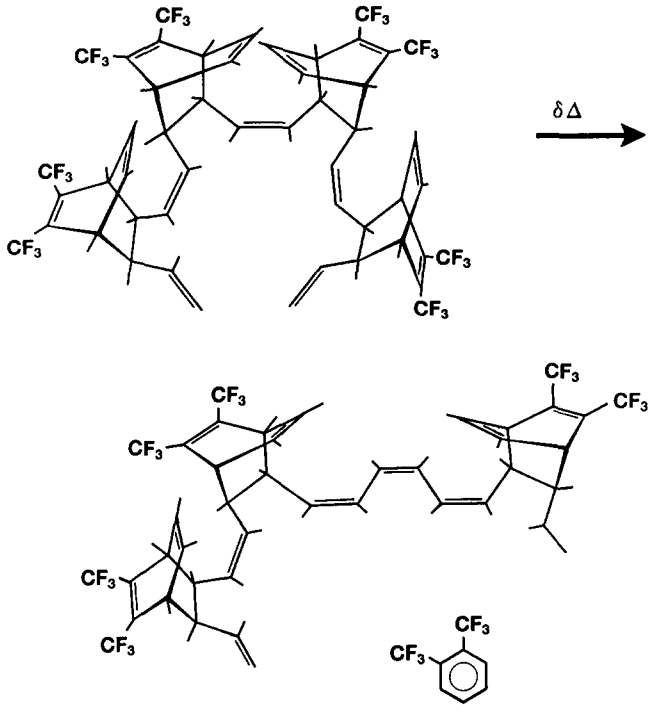

Figure 8 Effect of eliminated sequences in *cis*-meso precursor polymer chain

these materials and the assignment of carbon atoms are shown in *Figure 9*.

Several catalysts were successfully employed, generating a range of structures. Problems were encountered with the use of rhenium pentachloride ($ReCl_5$), a catalyst known to assemble very high *cis* content ring-opened metathesis polymers. *Figure 10* illustrates that key intermediates in the propagation reaction must also be very crowded sterically during the assembly of *cis* dyads.

The main conclusion of this study[3] was that the broad carbon-13 n.m.r. linewidths were principally due to stereochemical and conformational complexity. Each line was made up of the superposition of chemical shifts characteristic of the different environments a carbon at any one position could experience. These environments are due to the multiplicity of stereochemical and conformational relationships any one subunit can have with its nearest neighbours. Often, with polynorbornenes for example[5], only immediate neighbour effects can be resolved (e.g. cm and cr environments in dyads for allylic or vinylic main chain positions). If next nearest effects (e.g. cc and ct environments in triads) cannot be resolved, they would not normally be expected to generate the variety of shifts needed to produce the smooth broad resonance lines of the precursor polymer or (**I**). Therefore conformational effects need to be invoked as well, but, in line with the conclusions of the modelling exercise, they must be locked strongly into the chain to explain the invariance of the linewidth with temperature (20°C–100°C).

One further observation supports the significance of conformation. The carbon-13 n.m.r. was able to resolve the resonances from C(2, 3) allylic to *cis* and *trans* C1′–C2′ double bonds. The calculated *cis/trans* ratios agreed well with data from infra-red spectroscopy[11]. The width of all the n.m.r. lines could be correlated with the *cis* content of the polymer, the degree of broadening depending on assignment, and the least affected being C(11, 12). The lines which experienced most broadening were not those of the stereochemically most sensitive C(1′, 2′) and C(2, 3) positions, but those of C(1, 4). This observation could reflect a modification of the C(1,4) resonance positions brought about by steric compression of the bicyclic bridgehead as it is packed into highly crowded *cis* sequences in the polymer (*Figure 11*). The other positions experience a 'knock on' effect diminishing in size with remoteness from C(1, 4).

We suggest then, that the conformational constraints present in high *cis* materials are sufficient to induce a range of small structural modifications in the side groups, and these are manifested in the carbon-13 n.m.r. by line broadening. Since such energetically unfavourable effects can only be alleviated by coiling of the polymer, it follows that the materials that exhibit them are already tightly coiled.

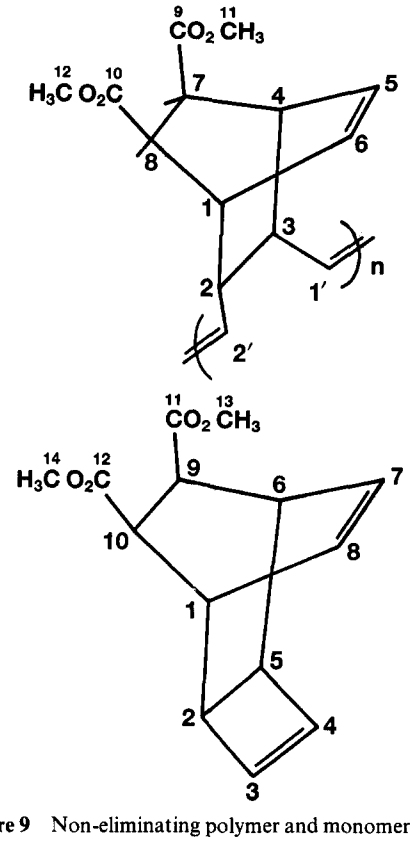

Figure 9 Non-eliminating polymer and monomer showing numbering system

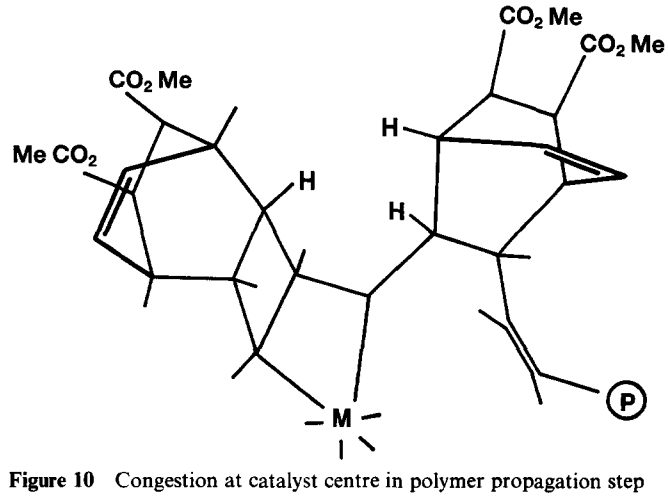

Figure 10 Congestion at catalyst centre in polymer propagation step

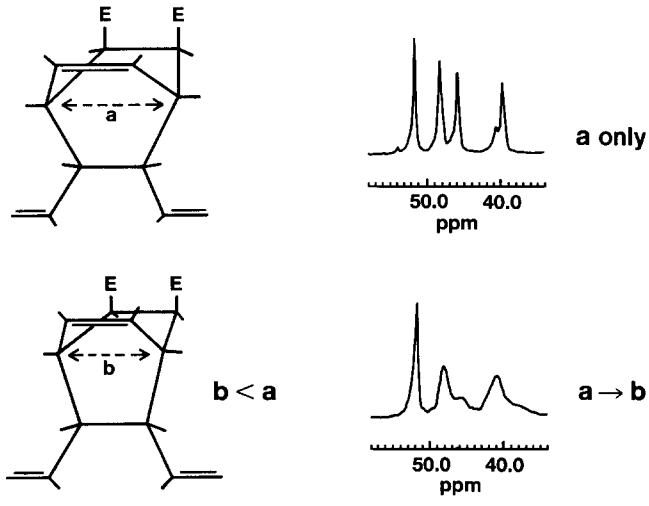

Figure 11 The effect of bridgehead flattening on n.m.r. spectrum

The carbon-13 n.m.r. linewidths of the precursor polymer are comparable to the broadest high *cis* lines for polymer (**I**). The precursor polymer is made with a tungsten hexachloride–tetramethyltin (WCl_6–Me_4Sn) catalyst which appears to give high *cis* (75–85%) microstructure[5], and is therefore expected to be highly coiled. As solutions of the precursor are warmed (40°C) and the elimination proceeds, resonances due to polyene sequences and 1,2-bis(trifluoromethyl)benzene appear but a significant change in the linewidth could not be detected. This observation implies either that the formation of polyene sequences does not relax the partially eliminated precursor structure, or that the elimination proceeds in a very blocky fashion.

(*1.4*) *Light scattering and gel permeation chromatography*

The precursor polymer is soluble in common solvents, which enables light scattering and g.p.c. to be performed. Weight-average molecular weights of 500 000–800 000 are typically recorded[8], corresponding to 2000–4000 double bonds in the polyacetylene. In tetrahydrofuran (at −27°C) the precursor polymer produced with the standard (WCl_6–Me_4Sn) catalyst elutes at a position similar to that of polystyrene of half the molecular weight. Hence the polymer chains are even more tightly coiled than those in polystyrene.

As yet it has not been possible to record equivalent information on a polymer with a higher *trans* content. It might be expected to have more open coils.

(2) CRYSTAL STRUCTURE

(*2.1*) *Introduction*

The hypothetical lowest energy state for polyacetylene is a perfect *trans* crystal. Polymerization of acetylene at above 150°C[9] gives a nascent fibrillar mat morphology and a para-crystalline *trans* structure, which cannot subsequently be modified using traditional polymer science since polyacetylene is intractable. Polymerization at −78°C[9] gives the *cis* isomer which can be isomerized thermally whilst preserving much of the order in a rather remarkable way. There is enough room for *trans* and *cis* units to exist within the same crystal structure, so that there is a smooth change from *cis* to *trans* character with no decrease in order.

The unique feature of the Durham route to polyacetylene is the amorphous precursor polymer which transforms to polyacetylene simply by heating.

The starting point is a film cast from a randomly coiled polymer in solution. From this film it is possible to obtain a wide range of structures. These structures vary from very slightly ordered, nearly amorphous *cis* polyacetylene through to a highly oriented, well ordered *trans* polyacetylene. These structures are described and, where necessary, compared with reported data on Shirakawa polyacetylene.

(*2.2*) *The precursor polymer*

Figure 12 shows a XRD scan of a precursor polymer made with a tungsten hexachloride/tetra methyl tin catalyst. It can be seen that the main peak is broad ($FWHM > 6°$) with a shoulder at higher angle arising from *cis* polyacetylene which has already started to form. There is also an extremely broad peak at ≃42°. This is more intense than usually is seen in amorphous polymers and results from the high fluorine content. *Figure 12* also shows how the structure evolves on transformation to polyacetylene. The main peak at ≃16° and the broad peak at ≃42° diminish in intensity and the shoulder grows to become the dominant feature. The coexistence of peaks from the precursor and polyacetylene suggest a two phase system, i.e. that the elimination reaction is not random. This is only consistent with the observed overall first order kinetics if it is the initiation which is the rate determining step and the propagation and termination steps for the elimination are both rapid.

All the lines in the carbon-13 magic-angle spinning solid state n.m.r. spectra of the precursor polymer were found to be broad (300–500 Hz compared to typical values for crystalline polymers such as polyethylene of 25 Hz). Solid state proton n.m.r. relaxation times were also found to be long ($T_1 \simeq 8$ s, $T_{1\rho} \simeq 50$ ms at −20°C).

These n.m.r. results, together with the lack of long range order evident from X-ray diffraction, indicate that the precursor is best described as an amorphous glassy polymer.

(*2.3*) *The structure of unoriented* cis *Durham polyacetylene*

On heating this amorphous precursor at 60°C for 60 min under vacuum 1,2-bis(trifluoromethyl)benzene is

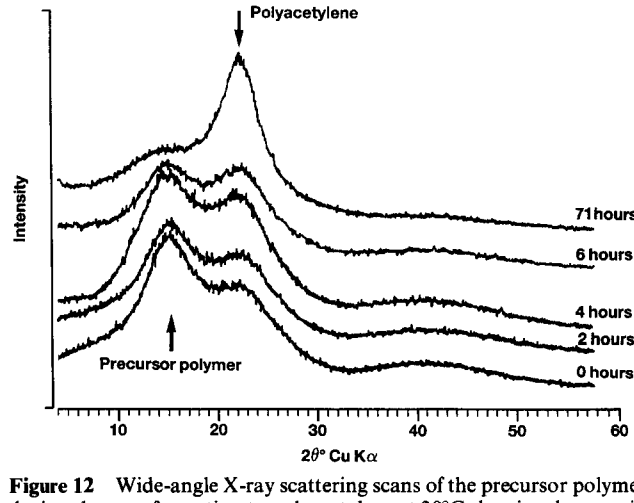

Figure 12 Wide-angle X-ray scattering scans of the precursor polymer during the transformation to polyacetylene at 30°C showing decrease in peak due to precursor and increase in peak due to polyacetylene

eliminated leaving predominantly *cis* polyacetylene[10]. (The exact fraction of *cis* depends on the fraction of *cis* double bonds present in the precursor as discussed in section (1.1), and on the limited amount of isomerization that occurs at 60°C. Further details of the elimination and isomerization kinetics are also given in ref. 11.) At this stage the polyacetylene still retains the amorphous character of the precursor (see *Figure 13*). The inter-chain peak is broad and any higher order peaks are weak and broad. The full width of the main peak at half height ($B_{1/2}$ is 4°(2θ CuKα), which corresponds to an apparent coherence length (L) of 2.2 nm using the Scherrer relationship (with $K=1$ and $\lambda=154$ pm; $B_{1/2}$ has not been corrected for instrumental broadening which is a very small correction for such broad peaks);

$$L=K\lambda/B_{1/2}\cos\theta$$

The Shirakawa polyacetylene peak is considerably narrower. (Baughman *et al.*[12], for example, have recorded a diffraction pattern from 85% *cis* polyacetylene in which the $B_{1/2}$ was approximately 1.5°, equivalent to a coherence length of 5.9 nm.)

The coherence length of predominantly *cis* Durham polyacetylene can also be compared to that of traditionally 'amorphous' polymers such as polyisobutylene ($L=2.0$ nm) and atactic polystyrene ($L=1.6$ nm)[10,13]. Thus if coherence length is taken as a measure of order, predominantly *cis* Durham polyacetylene lies between that of Shirakawa polyacetylene and traditionally 'amorphous' polymers.

The position of the inter-chain peak in predominantly *cis* Durham polyacetylene (22.6°, *d*-spacing 392 pm) is also at a lower angle than in Shirakawa polyacetylene (23.4°, 380 pm[12]). This implies that the Durham structure is less tightly packed therefore allowing more space for disorder.

(2.4) Structural changes during thermal isomerization

During isomerization Durham polyacetylene becomes more ordered. The changes in width of the inter-chain diffraction peak of Durham polyacetylene with time at 60°C, 90°C, 120°C are shown in *Figure 14*. Two features are apparent, firstly there is generally a decrease in $B_{1/2}$ with time (also observed for isomerization at 40°C, 80°C and 100°C but not shown) and secondly that the minimum width reached appears to be a function of temperature. This is shown more clearly in *Figure 15*

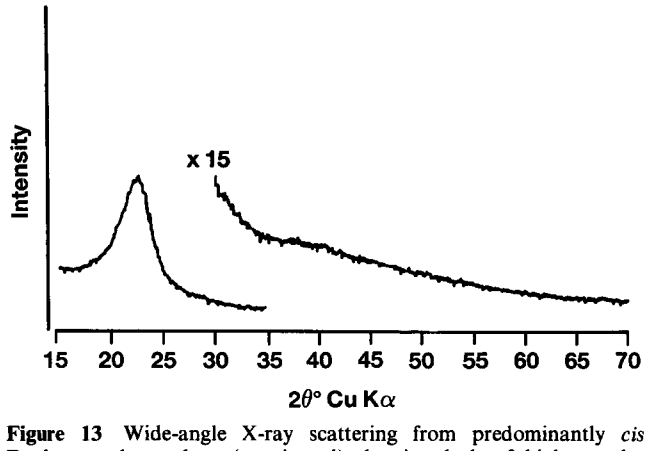

Figure 13 Wide-angle X-ray scattering from predominantly *cis* Durham polyacetylene (unoriented) showing lack of higher order structure

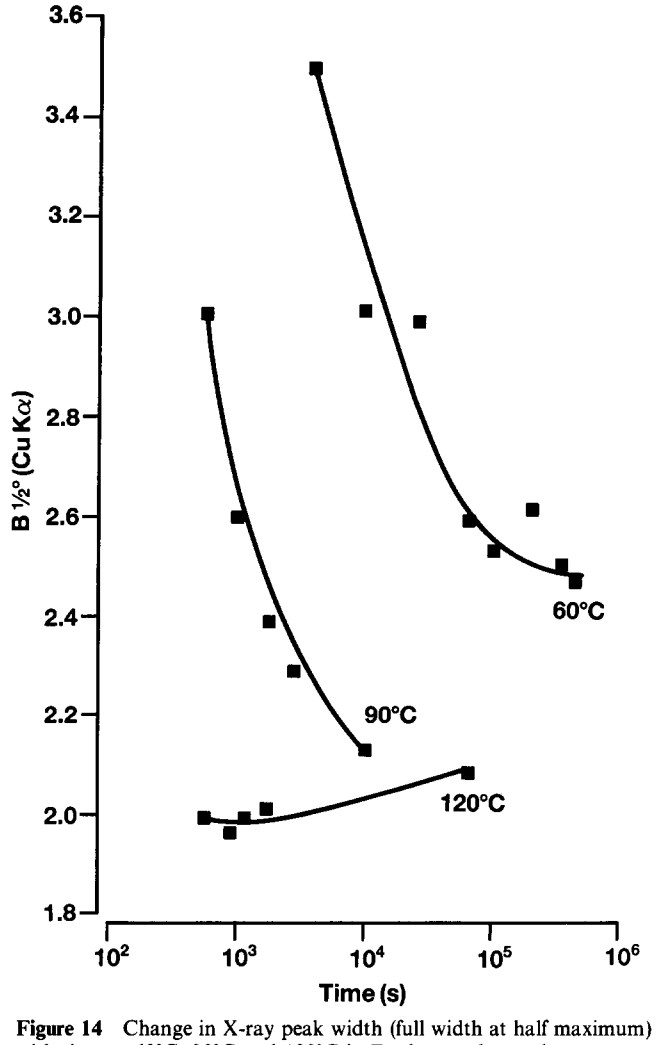

Figure 14 Change in X-ray peak width (full width at half maximum) with time at 60°C, 90°C and 120°C in Durham polyacetylene

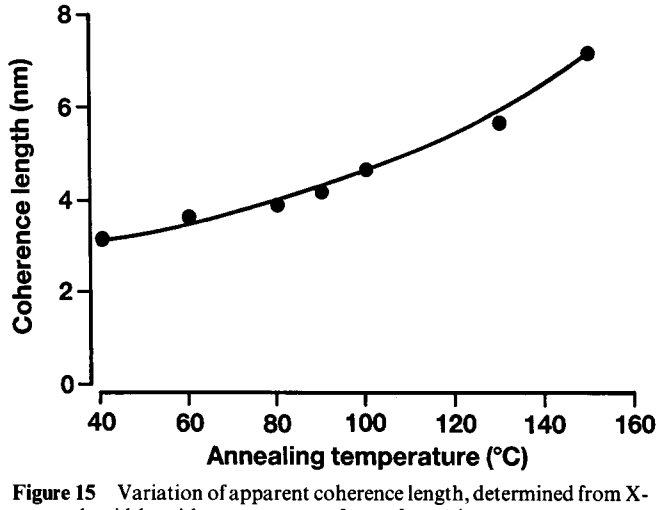

Figure 15 Variation of apparent coherence length, determined from X-ray peak width, with temperature of transformation

where the maximum observed coherence length (equivalent to minimum peak width) is plotted against temperature of transformation. This ordering is not seen in Shirakawa polyacetylene for three reasons; firstly, Shirakawa polyacetylene is already well ordered prior to isomerization, secondly, polyacetylene is very rigid so that large scale chain motions are precluded and thirdly there is no plasticizer present in Shirakawa polyacetylene. Hence, ordering during isomerization is not expected.

Indeed, it would be reasonable to predict that isomerization might introduce more defects into the structure. Robin *et al.*[14], in fact, reported no change in coherence length during isomerization at 150°C. (It should be noted that their value of 15 nm for L was later corrected to 7.5 nm[15]). Riekel[16] reported constant peak width followed by a slight increase (3%) in peak width at around 200°C on heating at 11°C/min. Pergero *et al.*[17] also observed little change in the width of the main reflection with isomerization.

However, the situation with Durham polyacetylene is different. Two factors contribute to the different behaviour of Durham polyacetylene. Firstly, the starting state is less ordered than *cis* Shirakawa polyacetylene and, secondly, there is evidence that residual 1,2-bis(trifluoromethyl)benzene acts as a plasticizing agent[11] for the isomerization. The magnitude of this effect is dependent on the film thickness. Diffusion control of the by-product loss means that thicker films show the effect of this plasticization more. It has previously been shown[11] that isomerization of Durham polyacetylene is more facile than in Shirakawa polyacetylene presumably for the same reasons.

Robin[14], Riekel[16] and Pergero[17] did, however, observe some other changes in X-ray diffraction during isomerization. They found a slow continuous shift in the inter-chain (200)/(110) peak position and no separate (*hk*0) reflections from distinct *cis* and *trans* crystals. They concluded that polyacetylene forms mixed crystals of *cis* and *trans* during isomerization. However, it can also be deduced from Pergero's data[17] that *trans* units do not

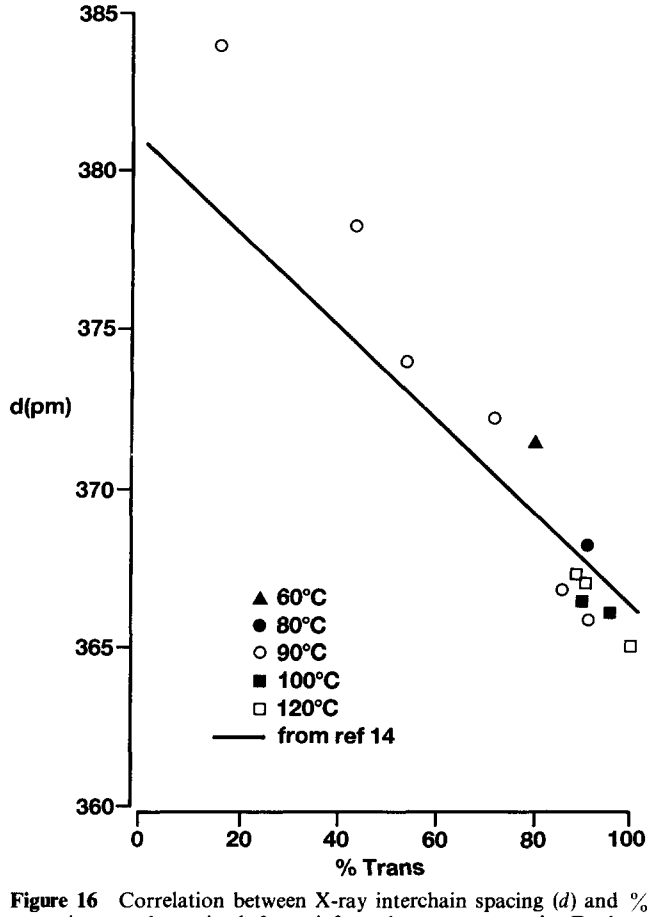

Figure 16 Correlation between X-ray interchain spacing (d) and % *trans* isomer determined from infra-red spectroscopy in Durham polyacetylene. The line for Shirakawa polyacetylene[14] is shown for comparison

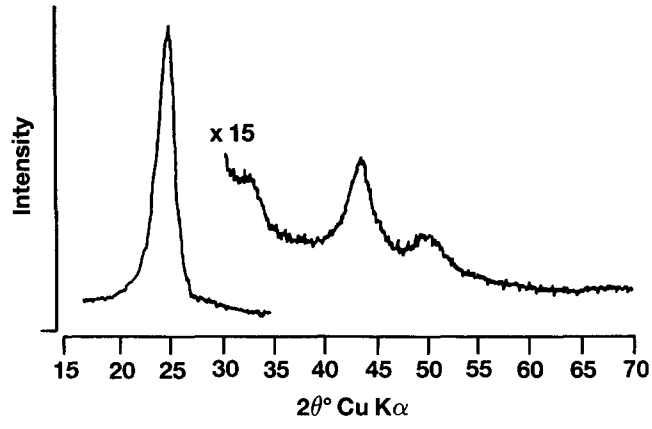

Figure 17 Wide-angle X-ray scattering from *trans* Durham polyacetylene (unoriented) showing higher order structure

form completely at random. Separate reflections from (002) *trans* and (004) *cis* are observed. Hence, separate *cis* and *trans* chains (or at least sections of chains longer than the coherence length) must co-exist in the same crystal. This is also suggested by the continuous linear shift in the (*hk*0) reflections since a completely random isomerization would not change the inter-chain spacing linearly. It would remain close to the *cis* value, held in place by the remaining *cis* until near the end of the isomerization when there would be a sharp reduction in d-spacing.

This shift in inter-chain spacing during isomerization is also observed in Durham polyacetylene (*Figure 16*). Furthermore, as in Shirakawa polyacetylene, no separate *cis* and *trans* (*hk*0) reflections were observed. Hence, it also seems to be the case for Durham polyacetylene that *cis* and *trans* chain segments co-exist in one continuous phase.

(*2.5*) *The structure of unoriented* trans *Durham polyacetylene*

The structure of *trans* Durham polyacetylene is a function of temperature. *Figure 15* showed that the coherence length (and hence the degree of order in the material) increased with temperature of transformation. No such trend has been observed for Shirakawa polyacetylene. The reported values for this coherence length in Shirakawa polyacetylene tend to be larger (7,5 nm in refs. 14 and 15, 6.3 nm in ref. 18 and 9.3 nm in ref. 19). *Figure 17* shows an X-ray diffraction scan of a sample of Durham polyacetylene transformed at 150°C. Four peaks are readily apparent which correspond to the (200)/(110), (210), (120)/(310)/(020) and (400)/(220) reflections of the Shirakawa unit cell[20]. The peaks become broader and less intense with increasing angle suggesting paracrystalline disorder, as with Shirakawa polyacetylene. The (210) reflection is not consistent with truly hexagonally packed chains, but the a^2/b^2 ratio is close to 3, the hexagonal value. This departure from hexagonal packing arises from the fact that the planar zig-zag of *trans* polyacetylene is not free to rotate. There is no evidence, in this sample, for splitting of the (200) and (110) but some indication of splitting has been seen in Durham polyacetylene[10]. This high temperature state is approaching that of Shirakawa polyacetylene.

The inter-chain d-spacing of *trans* Durham polyacetylene is not, however, a function of temperature of isomerization. *Figure 16* shows a cluster of points at greater than 80% *trans* whose temperature of

isomerization ranged from 60°C to 120°C. There is no distinguishable difference in *d*-spacing between the different temperatures of isomerization. The extrapolated value for fully *trans* Durham polyacetylene is around 365 pm which is in agreement with values for Shirakawa polyacetylene (365 pm[20] and 368 pm[21]).

(2.6) Orientation effects in Durham polyacetylene

It is possible to produce oriented Durham polyacetylene by stretching during transformation. This was first recognized when a film of precursor was transformed on a TEM grid and the diffraction pattern of the resultant polyacetylene recorded[22]. The diffraction pattern showed considerable orientation and a high degree of crystallinity and could be indexed according to the monoclinic cell of Fincher[20]. Subsequently, large areas of Durham polyacetylene have been oriented by stretching [23-26,11]. Sokolowski *et al.*[23] cast precursor films from acetone which they transformed to polyacetylene under a stress of about 600 N cm^{-2} at between 40°C and 60°C under vacuum, and subsequently at between 50°C and 100°C to complete the isomerization, obtaining draw ratios of up to 20. Leising[25] applied a stress of about 200 N cm^{-2} at temperatures up to 120°C achieving draw ratios of 10. We have oriented samples under constant velocity (25 μm s^{-1}) at 35°C–50°C under vacuum, obtaining draw ratios up to 25.

Predominantly *cis* Durham polyacetylene can also be oriented in a similar manner if the eliminated 1,2(bistrifluoromethyl)benzene is retained in the polyacetylene to act as a plasticizer. Thus it was found that *cis* samples could be oriented at room temperature, under nitrogen, with draw ratios up to 15 and *cis* content around 70%.

(2.7) The structure of oriented cis *polyacetylene*

Although the *cis* isomer is not thermally stable and its electrical properties are not as fully studied as those of the *trans* isomer, several publications[12,17,19,27-29,36] have discussed its structure based on unoriented or slightly oriented material. An orthorhombic unit cell with a space group of P_{nam} is agreed. Chien[27], for example, has reported unit cell dimensions of $a = 768$ pm, $b = 446$ pm, c(chain axis) = 438 pm, C–C–C angle 125°, a setting angle of 32° and 8 CH units per unit cell. This cell leads to distances between adjacent CH units, in the (110) plane, of only 27 pm which is less than the sum of the Van der Waals radii (18 + 17.7 = 29.7 pm). Chien suggested that

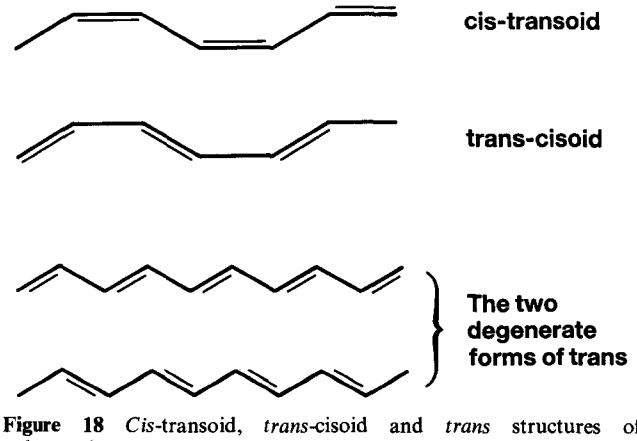

Figure 18 *Cis*-transoid, *trans*-cisoid and *trans* structures of polyacetylene

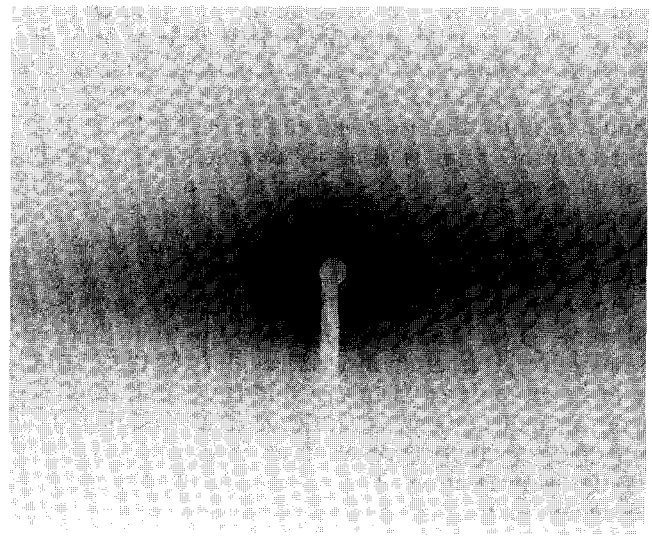

Figure 19 X-ray diffraction pattern of oriented predominantly *cis* polyacetylene (draw direction vertical)

this may explain the instability of the *cis* isomer. However, Baughman's unit cell[12] does not require this overlap. He estimated, from X-ray diffraction, $a = 761$ pm, $b = 439$ pm, $c = 447$ pm (chain axis) and setting angle of 39°.

The interchange of double and single bonds in *cis* polyacetylene leads to two non-degenerate structures, *trans*-cisoid and *cis*-transoid (*Figure 18*). Neither Baughman or Chien were able to differentiate between these two forms from their diffraction data. Packing calculations[12,18] have shown that the unit cell is only altered very slightly on going from *cis*-transoid to *trans*-cisoid. Spectroscopic data (see ref. 12 for discussion) tend to suggest a *cis*-transoid structure in Shirakawa polyacetylene. Ruland analysis of X-ray diffraction data[29] has yielded a relatively high value for crystallinity (76–84%) and a large degree of disorder within the 'crystals' ($k \simeq 5$).

An X-ray diffraction pattern of oriented Durham polyacetylene with $\simeq 60\%$ *cis* (*Figure 19*) shows higher orientation than is possible in Shirakawa material and a lower level of three dimensional order than oriented *trans* polyacetylene (see section (2.8)). In general there are no (*hkl*) reflections, but several streaks corresponding to repeat distances of 420, 216, 140, 119, 116, and 106 pm. The lines at 420, 216 and 106 pm can be indexed as *cis* (001)s and the 119 pm as *trans* (002). The line at 116 pm is intermediate between the *cis* (004) at 106 pm and the *trans* (002) at 119 pm, and is interpreted as coming from material which contains both *cis* and *trans* units. The lines at 116 and 140 pm do not correspond to a *cis* or *trans* repeat distance. The 140 pm reflection has also been observed by Chien[38] during the isomerization of Shirakawa polyacetylene and was denoted '?'. This peak was not present in either fully *trans* or fully *cis* polyacetylene and probably represents a strained intermediate conformation.

(2.8) The structure of oriented trans *polyacetylene*

The Durham route also enables coherent crystalline polyacetylene films to be produced. This material is of particular interest because it opens up the possibility of probing inter and intra-chain phenomena more deeply than is possible with the Shirakawa route. It is therefore

important to understand the structure of this material. Several publications have appeared[22-26,30,31] and will be compared with publications on Shirakawa polyacetylene and our own more recent results.

The production of fully *trans* oriented Durham polyacetylene requires more severe thermal treatment than does the unoriented material. *Figure 20* shows that significant amounts of *cis* are still present in oriented samples after 20 h at 90°C whereas the *cis* peak in unoriented Durham polyacetylene has practically disappeared. However, after treatment at 143°C for 5 h, under high vacuum, all the *cis* was removed (*Figure 21*). Leising also was not able to detect *cis* after 1 hour at 140°C. It is more difficult still to complete thermal isomerization of Shirakawa polyacetylene. For example Gibson *et al.*[32] found that 6.8% *cis* remained after 18 h at 180°C. However, fully *trans* Shirakawa polyacetylene can be prepared by polymerization at above 150°C[33]. Meyer[34] has polymerized acetylene under shear conditions giving highly aligned fibrils (but not solid films).

(2.8.1) The unit cell. Most of the data on Shirakawa polyacetylene support the view that the chain centres are packed pseudo-hexagonally, i.e. $a^2/b^2 \simeq 3$. (See *Table 1.*) The cylindrical symmetry of the chains (necessary for hexagonal packing) is, however, broken in two respects. Firstly, the planar zigzag conformation of the all *trans* polymer gives rise to reflections such as (210), which are not consistent with hexagonal packing. Various workers have also seen splitting of the main diffraction peak into (200) and (110) reflections[15,19-21,27] which is further evidence for a deviation from a hexagonal lattice. Therefore, there is correlation between the orientation of neighbouring planes of the zigzag and not free rotation (see *Figure 22*), leading to a herring-bone arrangement of chains as in polyethylene[35]. Fincher *et al.*[20] found the setting angle of the central chain to be 55° with respect to (010). This is close to the value predicted from packing calculations by Baughman[36] and those reported elsewhere (51°–60°) as shown in *Table 1.* (*h*00) and (0*k*0) reflections have not been observed when *h* and *k* are odd. The two dimensional space group is thus P_{gg}.

The second asymmetric feature of *trans* polyacetylene is the famous single/double bond alternation. If there is any

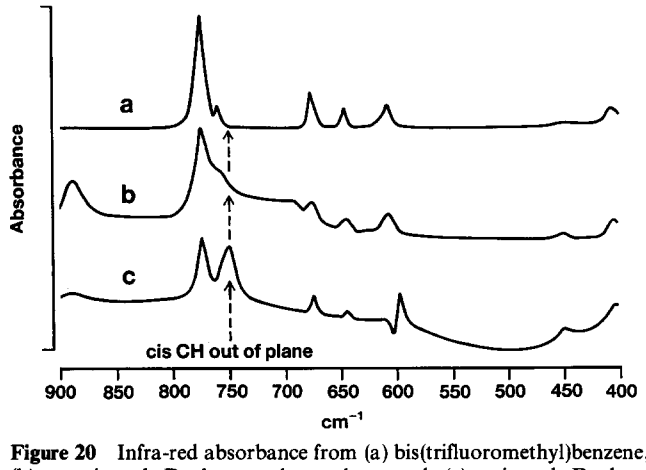

Figure 20 Infra-red absorbance from (a) bis(trifluoromethyl)benzene, (b) unoriented Durham polyacetylene and (c) oriented Durham polyacetylene after identical thermal treatment. The residual *cis* absorbance at ~750 cm^{-1} in the oriented sample illustrating that the increased order reduces the rate of isomerization significantly

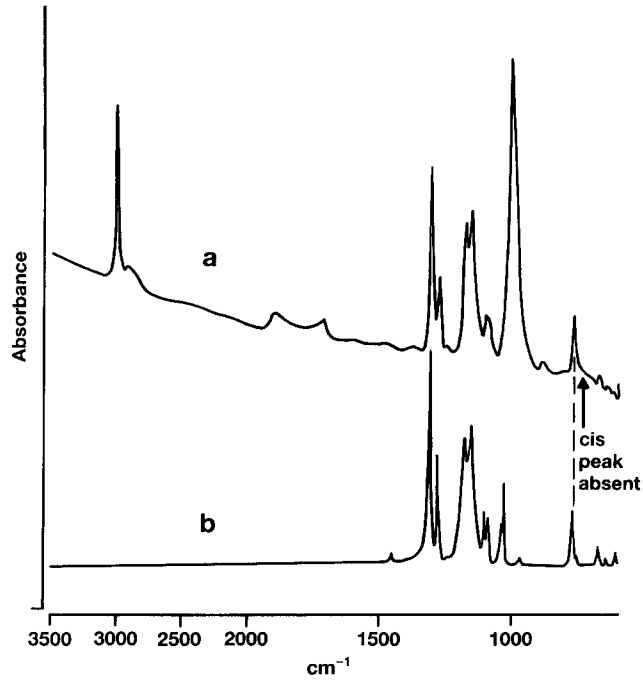

Figure 21 Infra-red absorbance of (a) oriented *trans* Durham polyacetylene (transformed at 143°C for 5 hours) and (b) bis(trifluoromethyl)benzene. The *cis* peak at ~750 cm^{-1} is now absent

non-random relation between the phase of these bond length alternations then the symmetry necessary for an orthorhombic unit cell is broken forcing the unit cell to be monoclinic. (See *Figures 22* and *23.*) Three phase relationships are conceivable; in phase (leading to space group $P2_1/a$), out of phase ($P2_1/n$) or random (equivalent to orthorhombic *Pnam*). The lowest energy state is the out of phase case. The (001) reflection is forbidden for the monoclinic out of phase relationship, but allowed for the random or in phase relationship. Fincher *et al.*[20] did not observe a (001) reflection suggesting the out of phase, $P2_1/n$, case. They calculated that if all the polyacetylene chains were in phase they would have had sufficient intensity to see a (001) reflection. From the position of the Bragg reflections they estimated a monoclinic angle between 91° and 93°. They also estimated the bond length alternation to be 3 pm[19,20]. However, Chien[37] observed a weak (001) reflection in electron diffraction. Thus he considered that the polyacetylene chains were in phase, although he did not comment on the possibility of a proportion of the chains being out of phase or of random phase relationship. From the ratio of the intensity of the (001) to (002) he estimated the bond length alternation to be 2.4 ± 0.2 pm. These two estimates of the bond length alternation can be compared to a measurement of 4 pm (leading to bondlengths of 144 and 136 pm) made by Yannoni *et al.*[38] using nutation ^{13}C n.m.r.

Leising *et al.*[24] have observed a very weak (001) reflection in Durham polyacetylene but it was not clear if this was the intensity of the layer line streak or a true peak in both the equatorial and meridional directions. We have observed a weak two dimensional (001) and layer line streaks[39]. These streaks are also visible in *Figures 24* and *25* which are X-ray and electron diffraction patterns of oriented Durham polyacetylene. Unit cells derived from these diffraction patterns are shown in the table. Note that a^2/b^2 is very close to 3 and no splitting of the (200)/(110) or of the (400)/(220) can be seen. (However, because

Table 1 Structural data on polyacetylene

Ref	Unit cell (pm)			a^2/b^2	[1]β	[2]ψ	[3]Density ($g\,cm^{-3}$)	Space group	[4]L_c (nm)	[5]Layer lines	[6]L_a (nm)	[7]Orientation	Crystallinity (%)	[8]Paracrystallinity	Comments
	a	b	c												
Shirakawa polyacetylene															
36x	741	408	—	3.30	91.3	51		$P2_1/a$							
33x													81	$k=5$	no SAXS peak
21e	732	424	246	2.98		24?	1.132	P_{nam}		3 s					(200)/(110) split
44n					95	54		$P2_1/a$			3–4		80–90		no (001)
37e															(001) seen
37e															C–C = ±2.4 pm
20x	732	424	246	2.98	91.5	55	1.130	$P2_1/n$	10	4	6.3	35°		$I_{004} \simeq I_{002}/4$	no (001), C–C = ±3 pm
17x	738	409	245.7	3.26		55	1.165								
14x	741	408	—	3.33											(200)/(110) split
15x	740	410	—	3.25		55			10–13		7/9				
19x											7.2 and 9.3		75–80		(200)/(110) split
45x								$P2_1/a$ and n			10			$p=15$ pm	
Durham polyacetylene															
23x	726	424	—	2.93					8		5	6°		$p=21$ pm	
24x									7.6	3 s					reflections at 734, 395 and 208 pm. (001) seen
26e	733	426	246	2.96	94.1		1.06								
30e	720	415	244	3.00			1.18			s		8°			
31e	734	418	234	3.08	90.5					6 s					(200)/(110) split and (001) seen
* x	727	420	243	2.99			1.14_5		3	2 s	5		approaching 100		isomerized at 143°C
* x	734	419	242	3.00					3	2 s	5		approaching 100		isomerized at 90°C
* e	724	419	243	2.99					5	6 s	5				isomerized at 100°C

Notes:
1 $\beta \neq 90°$ implies a monoclinic unit cell
2 ψ is the setting angle with respect to [010]
3 Densities are calculated from the unit cell except ref. 26 and this work, which are measured directly
4 L_c is the coherence length in the c (chain axis) direction, calculated from (002) widths
5 The highest order layer line observed, 's' indicates that streaks were observed at layer line positions
6 L_a is the coherence length in the a (or b) direction, calculated from (200)/(110) widths
7 Azimuthal Full Width at Half Maximum intensity of the (200)/(110) reflection
8 'k' is a disorder parameter ($k \simeq 2$ for polyethylene, see ref. 33, 'p' is a distortion parameter (see ref. 23))
9 'x' denotes X-ray diffraction, 'e' electron diffraction and 'n' neutron diffraction
* This work

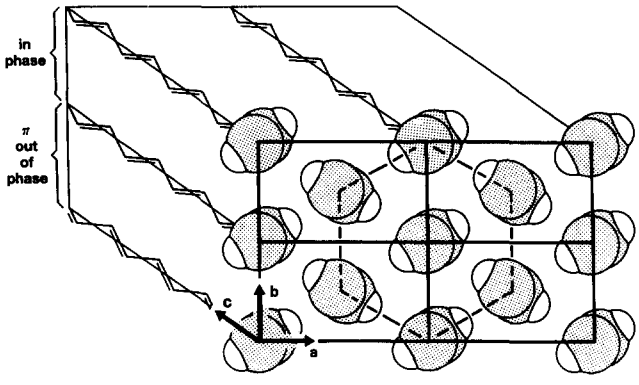

Figure 22 Schematic diagram of four unit cells of *trans* polyacetylene showing pseudo hexagonal packing and 'in phase' and 'π out of phase' relationships of the 'double' and 'single' bonds between nearest neighbours

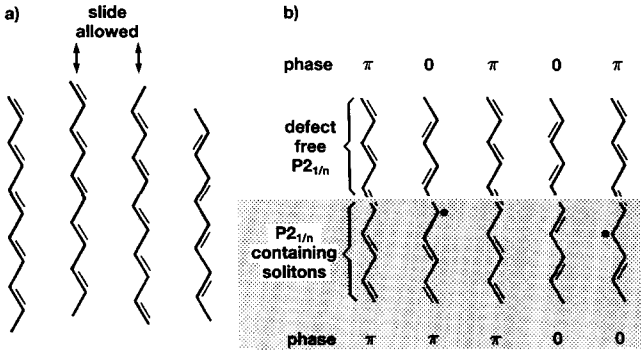

Figure 23 Schematic diagram of *trans* polyacetylene, (a) showing how nematic type disorder leads to no relationship between chains and (b) showing how solitons produce regions of 'in phase' material from a perfect $P2_1/n$ lattice (where the phase relation between chains is 'π out of phase'). These solitons would give rise to diffraction intensity at $l=1,3,5$ etc. which would not be present in a perfect crystal

the peaks are relatively broad any splitting is not expected to be resolvable.) Also note that the size of the unit cell seems to depend on transformation temperature, which is a similar effect to that seen in unoriented Durham polyacetylene (see section (2.4)).

Published dimensions of the *trans* polyacetylene unit cell are shown in *Table 1*. Densities calculated from these cells vary from 1.130 to 1.165 g cm^{-3} [17,20]. Leising measured a value of 1.06 g cm^{-3} [26] which does not appear to be consistent with the high crystallinity of oriented *trans* Durham polyacetylene. We have measured a value of 1.145 ± 0.01 g cm^{-3} for oriented *trans* Durham polyacetylene using a density gradient column[10], which appears to confirm the unit cell dimensions above. We found, however, the density of unoriented Durham polyacetylene (transformed below 100°C) to be 1.10 ± 0.01 g cm^{-3} which is consistent with its lower crystallinity.

(2.8.2) Possible types of disorder in oriented polyacetylene. The structure of polyacetylene is by no means fully described by the assignment of a lattice. It is perhaps more important, in order to understand electrical properties, to study how the structure differs from atoms on lattice points. Polyacetylene's departure from a perfect single crystal can be categorized into seven possible types of disorder.

(a) *Intramolecular disorder*

Either chemical or conformational intramolecular defects may exist in polyacetylene. Chemical defects might include crosslinks[40], chain ends, residual catalyst or precursor units and conformational defects may include residual *cis*, bends, kinks, solitons or polarons. Fincher[20] has predicted that solitons should lead to a diffuse sheet-like structure with a repeat distance of 246 pm along the chain, because solitons would disrupt any bond alternation phase correlation between chains (*Figure 23*). In general intramolecular defects will lead to meridional broadening of (001) reflections and a reduction in peak intensity with higher order layer lines.

(b) *Nematic disorder*

Nematic type disorder in polyacetylene would allow the chains to slide past each other without any correlation, between chains, of atomic positions in the chain direction (*Figure 22*). This would destroy any three dimensional reflections such as (121), so that

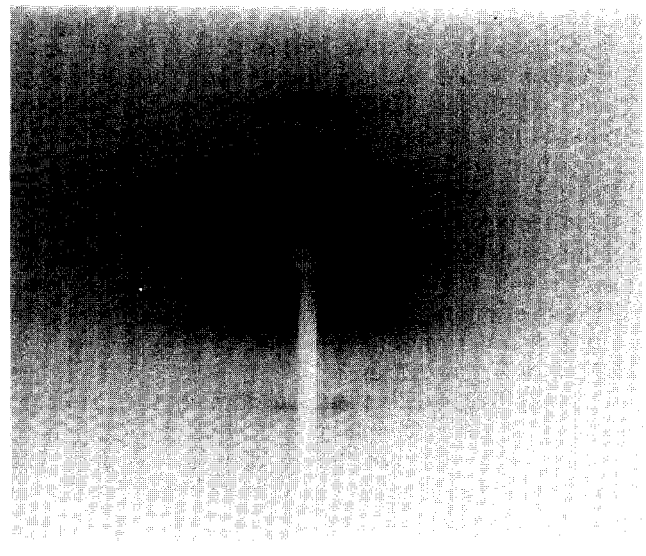

Figure 24 X-ray diffraction pattern of oriented *trans* Durham polyacetylene (draw direction vertical, draw ratio 23, isomerized at 80°C)

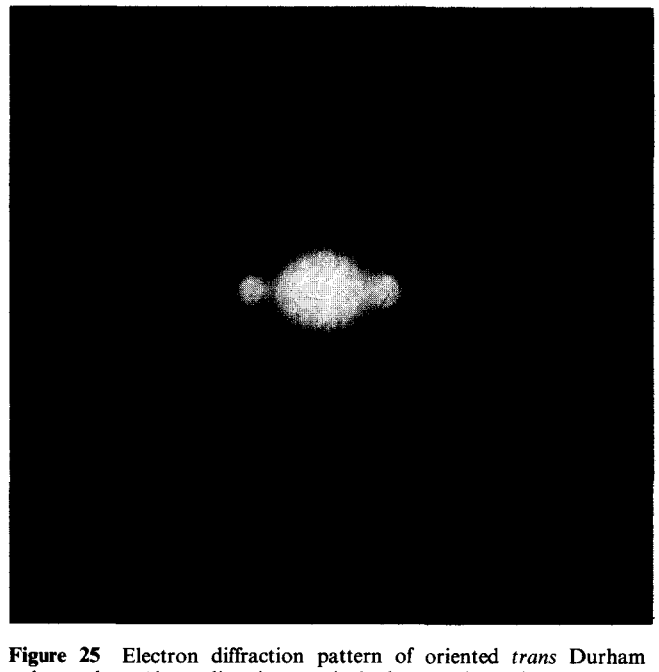

Figure 25 Electron diffraction pattern of oriented *trans* Durham polyacetylene (draw direction vertical, draw ratio 9, isomerized at 100°C)

layer lines would resemble streaks and contain no diffraction spots. This would be a more disordered state than the solitonic disorder described above, where there is correlation of atomic positions.

(c) *Orientation*
There will be a distribution of chain orientations centred on the draw direction. An indication of the orientation can be obtained from the azimuthal arcing of the (*hk*0) reflections. (Misorientation is not strictly a defect of the crystal structure, but is discussed here for completeness.)

(d) *Crystallinity*
There may be material that is not crystalline giving rise to an amorphous background to the diffraction pattern. It may also be possible to define a crystallinity in order to provide a guide to the total amount of order in the material, for example from density measurements. Alternatively, there may be a two phase structure, see (g).

(e) *Paracrystalline disorder*
Paracrystalline disorder perpendicular to the chain direction would give rise to equitorial broadening of (*hk*0) reflections. Higher order reflections would be reduced in intensity and further broadened.

(f) *Crystal boundaries*
Boundaries may exist between crystals, i.e. there may be inhomogeneity of crystal perfection giving rise to finite crystallite size broadening of (*hk*0) reflections, which will not broaden further at higher angles. Transmission electron microscopy is often used to study disorder of this type.

(g) *Multiphase structures*
If it is possible to define separate domains then a further type of disorder becomes conceivable. Two, or more, phases with different levels of order could exist concurrently. The phases could be differentiated with respect to any of the above types of disorder (except (f)). The two phase structure of polyethylene is an example of this. Multiphase structures are generally studied by SAXS or neutron scattering.

In addition to these types of disorder the fibrillar morphology of Shirakawa polyacetylene should also be considered.

(2.8.3) Types of disorder observed by diffraction methods. In comparison to inorganic semiconductors there are many more defects in polyacetylene and much less is known about them. Detailed study of defects in polyacetylene, however, is probably as important as in inorganic semiconductors, since 'defects' such as solitons are believed to carry the charge and other types of defects are likely to limit the electrical conductivity.

The morphology of Shirakawa polyacetylene makes the study of these different types of disorder difficult, but this has not prevented several publications appearing. *Table 1* summarizes, under the six headings outlined above, published data on Shirakawa and Durham polyacetylene.

Firstly the coherence length parallel to the chains (L_c) of Shirakawa polyacetylene has been measured by Fincher[20] from the (002) reflection to be 10 nm and Pouget[15] has reported a range from 10–13 nm. For Durham polyacetylene Leisling[24] shows a peak at (002) of width 1.5° (equivalent to $L_c = 7.7$ nm) and Sokolowski[23] reported a value of ~8 nm for L_c. The width of the (002) in *Figure 24* is 1.32° (2θ MoKα) ($L_c \simeq 3.3$ nm). A coherence length of 8 nm, for instance, represents an average of 65 carbon atoms between defects along the chain. Some defects, however, would be expected to destroy coherence more drastically than others. Crosslinks, for example, might be expected to be more destructive than solitons. From the shape of the (002) reflection it is possible, in theory at least, to determine the distribution of coherence lengths, but this has not yet been attempted. Resonance Raman spectroscopy can also probe the effective length of undisturbed conjugation, but the absolute values are rather dependent on the model assumed and, interestingly, on the type of defect[41]. A bimodal distribution of conjugated sequence lengths has often been seen in both Shirakawa and Durham polyacetylene peaking at ~9 and ~40 carbon atoms[42,43]. The larger X-ray values probably reflect both the type of average taken in converting X-ray peak widths to coherence lengths (which gives more weight to longer sequences) and the use of peak widths at half height instead of integral widths (which would reduce the estimated coherence lengths). Also X-ray diffraction is probably less sensitive than Raman to disruption of chain perfection.

Order parallel to the chain is also reflected by the number and intensity of the layer lines. Fincher[20] has observed a (004) reflection about four times less intense than the (002). Leising has seen six layer lines in Durham polyacetylene. Four layer lines are visible in *Figure 25*. The $l = 1$ layer line consists of a superposition of Bragg arcs on a streaky background. Leising has also reported streaky layer lines. There is a general reduction in layer line intensity with angle, but also an odd even effect. The odd layer line streaks ($l = 1$ and 3) are weaker than the even ($l = 2$ and 4). This odd even effect cannot be explained by nematic disorder alone (see *Figure 23*). However, solitons disrupting a $P2_1/n$ space group could explain this effect. The general reduction in intensity with angle is expected from the limited coherence along the chain.

Durham polyacetylene is considerably easier to orient than Shirakawa polyacetylene. Stretched Shirakawa polyacetylene has a meridional (200)/(100) arc of 35° (*FWHM*), at best. This arcing reduces to 6° or 8° for Durham polyacetylene[23,27]. The anisotropy of the *trans* infra-red absorption at 1010 cm^{-1} and the optical absorbance anisotropy at 2 eV are also extremely high[24,25]. Orientation of Durham polyacetylene does not appear, by X-ray diffraction, to be a very sensitive function of draw ratio. Draw ratios above ~5 do not change the azimuthal arcing appreciably[23]. However, we have found that other properties, such as e.s.r. line width, do change with higher draw ratios. This probably arises because the azimuthal width of X-ray (200)/(110) peak simply gives one type of average orientation and no information about orientation distribution. It may be the tails of this distribution that determine the conductivity and e.s.r. spectra of the oriented polyacetylene rather than an average.

The crystallinity of Shirakawa polyacetylene has been reported to be ~80% (using Ruland analysis[29]), 75–80% (from deconvoluting the 'amorphous' and 'crystalline' peaks from X-ray diffraction[19]) and 80–90% (from neutron scattering intensities[44]). The usual problem of the definition of crystallinity in a pseudo-one phase material arises. It is an over simplification to try to describe all the above types of disorder in one parameter.

Nevertheless, there is undoubtedly very little completely disordered and unoriented polyacetylene present in the samples. A different approach is to compare the measured density with that calculated from the unit cell dimensions. Accurate densities have only been reported for Durham polyacetylene. Brown *et al.*[10] reported a value of $1.145 \pm 0.01\ g\ cm^{-1}$, very close to the unit cell density ($1.13–1.165\ g\ cm^{-1}$). The densities of amorphous polymers are typically 85–90% of crystalline densities[10]. Liesing[26] reported a value of $1.06\ g\ cm^{-1}$, which is approximately half way between the hypothetical crystalline and amorphous densities, much lower than expected.

There is considerable evidence for paracrystalline disorder in polyacetylene. Estimates of the coherence perpendicular to the chains (L_c) have been measured from the widths of (200)/(110) reflections. They vary from 3 nm[26] to 10 nm[45] for Shirakawa polyacetylene (see *Table 1*). There are two possible origins of this broadening; either paracrystallinity or finite crystallite size. In principle it is possible to distinguish between these two effects since the square of the width of the peak should vary as the 4th power of the scattering vector for paracrystalline disorder whereas it should be unchanged for finite crystallite size broadening[23]. This can only strictly be done on single peaks, but if $a^2/b^2 \simeq 3$ then broadening from peak doubling can be ignored. Pouget[45] has shown increasing widths with scattering vector and has reported an extrapolated crystallite size of ~10 nm. Sokolowski *et al.*[23] have compared Pouget's data on Shirakawa polyacetylene with their data on Durham polyacetylene. They find that Durham polyacetylene has a smaller apparent crystallite size (5 nm compared to 10 nm for Shirakawa polyacetylene) and a larger paracrystalline distortion parameter (2.1 pm compared to 1.5 in Shirakawa polyacetylene). Fincher[20] suggested that the fibril dimensions (~20–50 nm) in Shirakawa polyacetylene might contribute to the broadening but since the measured coherence lengths are all smaller than 20 nm this is probably not a major contribution to the broadening.

It might be expected that inhomogeneity of crystal perfection (apparent crystallite size ~5 nm in Durham polyacetylene) might lead to a detectable SAXS peak if there is a two-phase structure. However, Brown *et al.*[10] did not detect such a peak from *unoriented* Durham polyacetylene in the region 1 to 8 nm. This may simply be because of the lower crystallinity of unoriented Durham polyacetylene.

(3) DISORDER AND DOPING IN DURHAM POLYACETYLENE

(3.1) *Introduction*

It is the ability of polyacetylene to be doped to high conductivities that has caused the considerable interest in this material in recent years. Doping causes gross electronic, optical and structural changes to occur in polyacetylene and can effectively be achieved by either chemical or, more favourably, electrochemical methods.

Chemical doping is normally carried out by exposure of the polyacetylene to electron-withdrawing compounds such as AsF_5 and SbF_5 to oxidize the polyacetylene and produce 'p'-type doped material, or by exposure to electron-dominating compounds such as n-butyl lithium and sodium napthalide to reduce the polyacetylene and produce 'n'-type doped samples. However, chemical doping, even if carried out with extreme care, can lead to dopant inhomogeneity.

Electrochemical methods on the other hand allow improved dopant homogeneity and give very effective fine control of dopant concentration. This control has been exploited by research groups to gain insight into the intrinsic and subtle electronic and structural changes occurring in polyacetylene during the doping process.

One of the best electrochemical methods appplied to the study of polyacetylene is electrochemical voltage spectroscopy (EVS). This voltage step technique was first described in a series of papers by Thompson[46–49] and was used initially to investigate the lithium intercalation reaction in inorganic layered structure materials such as TiS_2 and V_2O_5. EVS provides a high resolution approximation to the open circuit discharge curves often reported for conducting polymer systems (i.e. the relationship between charge transferred, Q at a particular fixed potential, V). The V *versus* Q curve and its derivative, the dQ/dV *versus* V plot can yield important structural and thermodynamic information. For instance an inflection in the V *versus* Q curve is normally indicative of multi-phase behaviour for the conducting polymer whereas regions of changing voltage represent ranges of homogeneity within a single phase. The scope of the EVS technique can also be extended to allow the determination of kinetic information such as the electrochemical diffusion coefficient, D. This can be calculated at each voltage step by monitoring the decay of the cell current which is normally proportional to $t^{-1/2}$ for linear diffusion in a semi-infinite system[50].

(3.2) *Bandtailing in unoriented Durham polyacetylene*

The 'n'- and 'p'-type EVS plots for unoriented Durham polyacetylene between 0 and 0.5 mol % doping concentration for Li^+ and ClO_4^- respectively are shown in *Figure 26*. Injection of the dopant ions occurs to maintain electroneutrality by counter-balancing the number of electrons injected into ('n'-type) or ejected from ('p'-type) the polyacetylene electrode. The first important point to note from inspection of the Figure is that the two plots are non-symmetric. This implies that the inclusion of the dopant ions causes some structural rearrangement and that the shape of the plot is dependent on the dopant ionic size and its degree of solvation. This last point is of particular importance since it has been clearly demonstrated that for Li^+ doping in a THF based electrolyte that the dopant ion is highly solvated[51].

Since the electrochemical doping of polyacetylene is achieved by single electron transfer the Figure effectively represents the energy level (*versus* some reference, in this case Li/Li^+) of the electronic states around the band edge. It can be clearly seen that there exists considerable 'tailing' of both the 'n'- and 'p'-doping plots. This situation arises from the fact that there exists a large number of available electronic states within what is normally considered the band gap. Deep tails such as these only arise from a gross density of such defect states. We therefore conclude that the unoriented Durham polyacetylene which has low crystalline nature, possesses a high density of such defects at energies around the band edge. This situation is analogous to that of the conventional semiconductor material, amorphous silicon which possesses a relatively high defect concentration

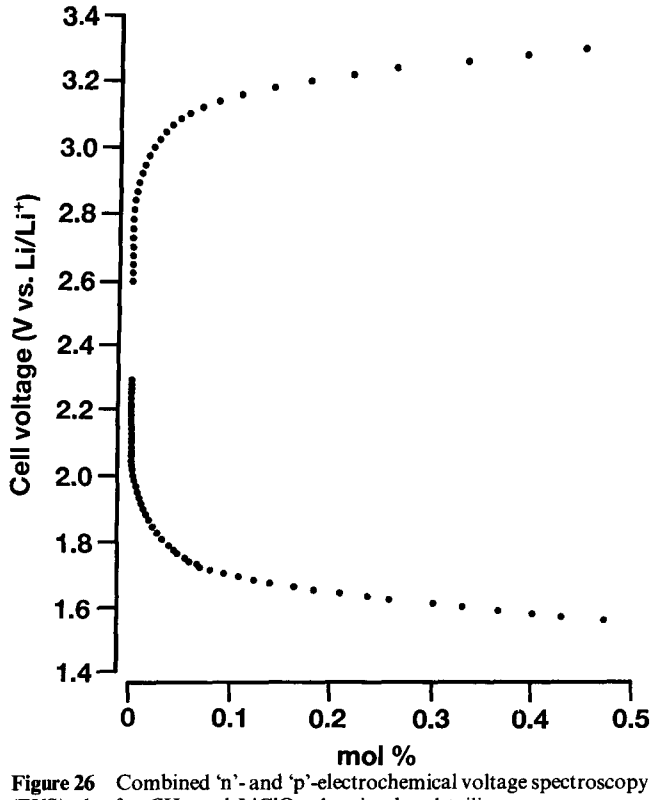

Figure 26 Combined 'n'- and 'p'-electrochemical voltage spectroscopy (EVS) plot for CH_x and $LiClO_4$ showing band-tailing

(compared to crystalline silicon) and consequently shows considerable band edge tailing[52].

(3.3) The effect of increased order on band-tailing

Figure 27 shows a comparative EVS data for the Na^+ doping in oriented and unoriented Durham polyacetylene over the restricted concentration range 0 to 0.1 mol% Na^+. There exists considerable band-tailing for the sodium doping process in the unoriented material in a similar way to that which has already been demonstrated for Li^+ in this material in *Figure 26*. However, the plot for the highly oriented material is noticeably different showing far less tailing and a main dopant injection threshold at higher potential (around 0.1 V higher than the unoriented material). This implies a smaller range of electronic energy levels is available around the band edge for the far more crystalline oriented material. This condition generates a far clearer band edge threshold due to a far smaller concentration of mid-gap defect states.

(3.4) The effect of order on doping to higher levels

E.s.r. measurements carried out *in situ* during electrochemical Na^+ doping of Shirakawa polyacetylene have implied there exists a sharp first order phase transition at a doping concentration of approximately 6 mol%[53,54]. At this transition it is argued that the electronic conduction mechanism changes from spinless soliton motion to a metallic type conduction. Separate EVS[51] and X-ray diffraction[55,56] measurements have confirmed this transition in terms of not only an electronic change but also a structural rearrangement of the $(CH)_x$ chains.

This structural transition has also recently been shown to exist for the alkali-metal dopant species such as K^+ and Rb^+ (but not for Li^+ which is considered too small to 'stabilize' the doped polyacetylene structure). It is considered that the polyacetylene chains are fairly readily rearranged during the doping process by the alkali metal ions such that a channel-like structure is formed. Shacklette and coworkers[55] argue that the in-coming alkali ions then become accommodated in these channels, until at around 6 mol% they form a 'superlattice' (ions all equidistant within the channels). A preliminary *in-situ* X-ray diffraction investigation on oriented Durham polyacetylene during an electrochemical doping cycle has now been undertaken[39]. This study has provided evidence for both chain rearrangement and sodium ion ordering (along the chain direction) during the doping process.

It is reported from e.s.r. studies that the abrupt electronic transition only occurs in well ordered systems and that the data is easily 'smeared' by disorder present in the polyacetylene[54]. Unoriented Durham polyacetylene is known to be considerably disordered and it can be visualized that the transition in this case be 'smeared'. The EVS data presented in *Figure 28* for the Na^+ doping of the unoriented material indeed shows a smeared out inflection around 6 mol%. The unoriented material only possesses 'local' ordering with only short straight sequences of CH chain units such that only localized channel structures can be obtained to accommodate the alkali metal dopant ions. From inspection of the EVS data it can be deduced that there must exist a relatively wide range of energies at which these localized structures can be reached by the dopant ions, presumably dependent on their relative position, size and ease of access.

In contrast to the unoriented material the oriented Durham polyacetylene is well ordered and possesses long

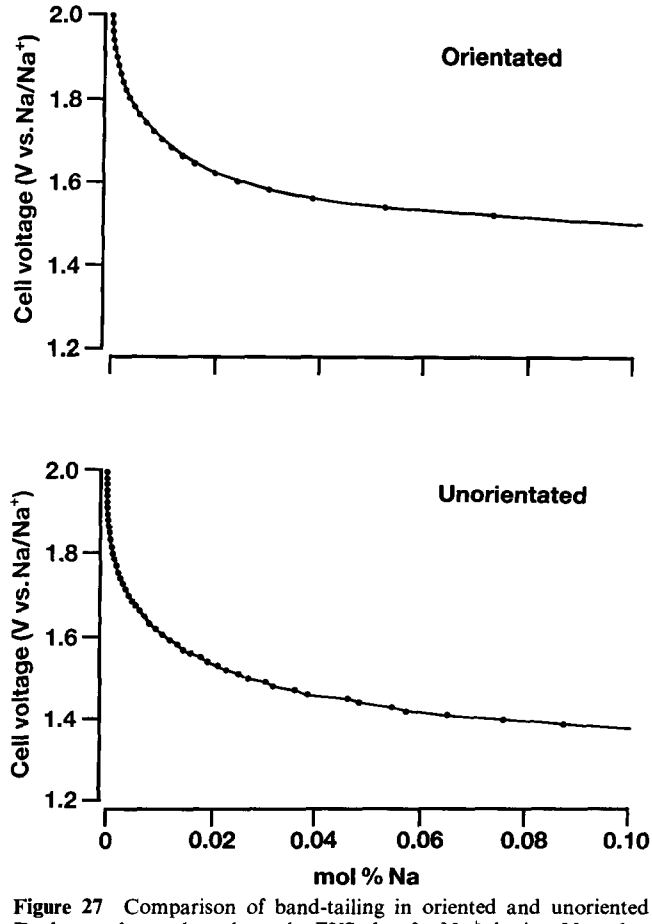

Figure 27 Comparison of band-tailing in oriented and unoriented Durham polyacetylene shown by EVS plots for Na^+ doping. Note that the equilibrium voltage is higher for the oriented material

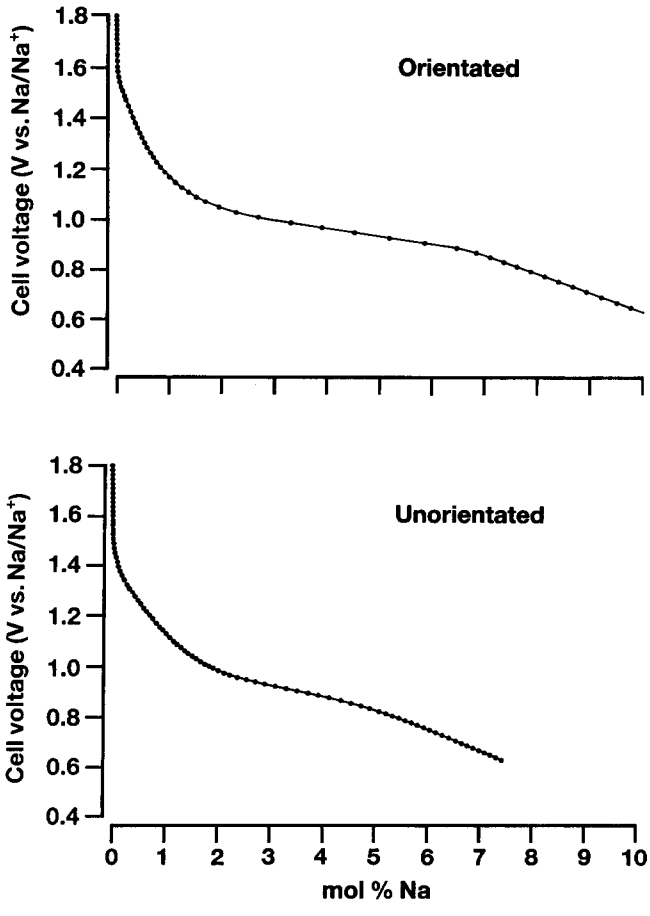

Figure 28 0–10% doping for oriented and unoriented Durham polyacetylene showing sharpening of inflection at 6% transition

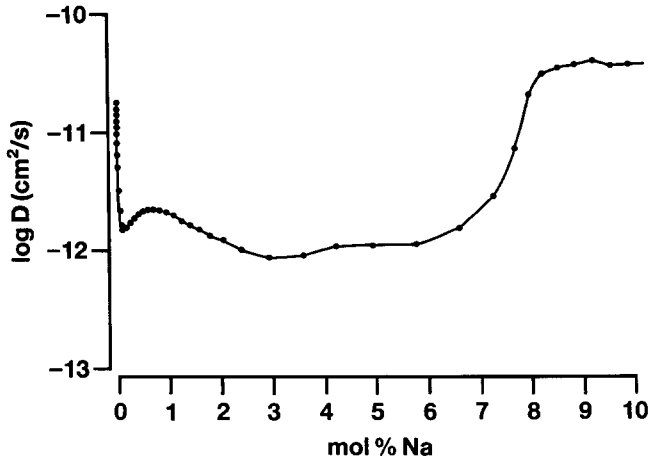

Figure 29 Variation of electrochemical diffusion coefficient, D with dopant concentration for oriented Durham polyacetylene showing change in diffusion coefficient at 6% transition

range order along the chain direction (see section (2.8.3)). This condition should allow the formation of long range sodium ion ordering along the chain direction and hence a well-defined transition in EVS data. In fact the EVS data presented in *Figure 28* indeed shows a sharp inflection at around 6 mol% Na^+, 850 mV *versus* Na/Na^+. We therefore conclude that, as predicted, the well ordered, oriented material allows the formation of considerable sodium ordering. Further electrochemical evidence for this structural ordering can be inferred from *Figure 29* which shows the variation in electrochemical diffucion coefficient, D against dopant concentration at 20°C. From inspection it can be seen that between 1 and 6 mol% Na^+ the value of D is fairly constant, whereas between 6 and 8 mol% there is an increase in D from around 1×10^{-12} cm s^{-1} to 5×10^{-11} cm^2 s^{-1}. We conclude that this dramatic increase in D may well arise from the onset of structural ordering whereby all the channels have been 'accessed' and in-coming Na^+ can then diffuse relatively rapidly.

(4) CONCLUSIONS

The n.m.r. results in section (1) strongly suggest that the precursor polymer does not possess an ordered microstructure. The correlation between the overall structure of the precursor and that of the product polyacetylene is, therefore, not easy to define. Modelling, and a fair amount of lateral thinking, suggests that it might be possible to control the precursor microstructure and thereby influence the ordering in the product polyacetylene, but, as yet, this is not possible.

The effect of transformation conditions on the crystal structure of the polyacetylene is more easily probed and hence the mechanisms are better understood. The development of more ordered structures at higher transformation temperatures is a consequence of the sequential reactions involved in the overall 'transformation' reaction. Film thickness also plays a role, by introducing the diffusion control of plasticizing by-product loss as a factor. By variation of the transformation conditions it is therefore possible to produce a limited range of isotropic structures.

Perhaps the most interesting structure to be produced by the Durham route is the oriented material. The orientation and consequent increase in crystallinity is familiar to polymer scientists, but the complexity of the processes involved make the continuing work on polyethylene look simple by comparison. It is necessary to heat the precursor slightly to facilitate drawing, and this heating causes transformation during the stretching process. The conditions used are therefore crucial to balance the physical and chemical processes. The understanding of the electronic effects in these oriented films is still not complete, though in general it can be stated that the dependence of different properties (conductivity, optical absorption, resonance Raman lineshape, e.s.r. linewidth, etc.) on draw ratio (as a rough measure of order) is not the same.

The effect of the order of the system on the doping characteristics of the polymer and the reciprocal effect of doping on the order are the visible manifestations of the complexity of the system. It has been noted elsewhere[41] that the strong disorder present in the unoriented material produces major optical effects on the polyacetylene. Whereas Shirakawa and oriented Durham material show a band gap of around 1.5 eV and a band maximum at 1.9 eV, in the unoriented material this band, maximum, in particular, is shifted to higher energies, sometimes by as much as 0.4 eV. This can be explained, along with a broadening of the e.s.r. linewidth, by invoking shorter conjugation lengths. These shorter conjugation lengths are a consequence of the increased disorder in the unoriented material. This can be demonstrated by orienting the precursor, where all the optical and electronic properties improve. The formation of band tails with increased disorder is an interesting possibility, and bears further investigation.

Overall the picture of order in Durham route polyacetylene is a complex one. There is the possibility of the chemical structure of the precursor affecting the product. There is proof that the transformation conditions used have a large effect on the crystallinity, and simply stretching the precursor during transformation produces a dramatically different material. Finally there are the strong effects of the ordering of the pristine polyacetylene on the doping process and evidence for a structural phase transition at the 6% doping level associated with the 'semiconductor-to-metal' transition.

ACKNOWLEDGEMENTS

The authors would like to thank all those who have contributed to the work discussed in this paper. In particular, Paul Calvert, Mike Taylor, Gordon Parkinson, Subramanian Ramdas, Mary Vickers and Nick Walker have provided us with many valuable insights into both these materials and the techniques used to investigate them. They would also like to thank British Petroleum p.l.c. for permission to publish this paper.

REFERENCES

1 Edwards, J. H., Feast, W. J. and Bott, D. C. *Polymer* 1984, **25**, 395
2 'Developments in Polymer Degradation—3', Ed. N. Grassie, Applied Science (1981), p. 122
3 Feast, W. J., Taylor, M. J. and Winter, J. N. *Polymer* 1987, **28**, in press
4 Williams, K. P. J., Gerrard, D. L., Bott, D. C. and Chai, C. K. *Mol. Cryst. Liq. Cryst.* 1985, **117**, 23
5 Ivin, K. J. 'Olefin Metathesis', J. Wiley, New York (1983)
6 ChemGraf created by E. K. Davies, Chemical Crystallography Laboratory, Oxford University, developed and distributed by Chemical Design Ltd, Oxford
7 Filipini, G., Induni, G. and Simonetta, M. *Acta Cryst.* 1973, **B29**, 2471
8 Harper, K. and James, P. G. *Mol. Cryst. Liq. Cryst.* 1985, **117**, 55
9 Ito, T., Shirakawa, H. and Ikeda, S. *J. Polym. Sci. Polym Chem.* Edn, 1974, **21**, 11
10 Brown, C. S., Vickers, M. E., Foot, P. J. S., Billingham, N. C. and Calvert, P. D. *Polymer* 1986, **27**, 1719
11 Foot, P. J. S., Calvert, P. D., Billingham, N. C., Brown, C. S., Walker, N. S. and James, D. I. *Polymer* 1986, **27**, 448
12 Baughman, R. H., Hsu, S. L., Pez, P. G. and Signorelli, A. J. *J. Chem. Phys.* 1978, **68**(12), 5405
13 Turley, J. W. 'X-ray Diffraction Patterns of Polymers', Dow Chemical Co., Midland, Mich., 1965
14 Robin, P., Pouget, J. P., Comes, R., Gibson, H. W. and Epstein, A. J. *Phys, Rev. B* 1983, **27**, 3938
15 Pouget, J. P., Robin, P., Comes, R., Gibson, H. W., Epstein, A. J. and Billard, D. *Physica* 1984, **127b**, 158
16 Riekel, C. *Makromol. Chem., Rapid Commun.* 1983, **4**, 479
17 Perero, G., Lugi, G., Pedritti, U. and Cernia, E. *J. de Physique* 1983, **44**(C3), 93
18 Fincher, C. R. Jr., Moses, D., Heeger, A. J. and MacDiarmid, A. G., *Synth. Met.* 1983, **6**, 243
19 Haberkorn, H., Naarman, H., Penzien, K., Schlag, J. and Simak, P. *Synth. Met.* 1982, **5**, 51
20 Fincher, C. R. Jr., Chen, C. E., Heeger, A. J., MacDiarmid, A. G. and Hastings, J. B. *Phys. Rev. Lett.* 1982, **48**(2), 100
21 Shimamura, K., Karasz, F. E., Hirsch, J. A. and Chien, J. C. W. *Makromol. Rapid Commun.* 1981, **4**, 477
22 White, D. and Bott, D. C. *Polymer* 1984, **25** (*Commun.*), 98
23 Sokolowski, M. M., Marseglia, E. A. and Friend, R. H. *Polymer* 1986, **27**, 1725
24 Leising, G., Kahlert, H. and Leitner, O. in 'Electronic Properties of Polymers and Related Compounds (Solid-State Sciences 63)', Springer, Berlin 1985, p. 56
25 Leising, G. *Polym. Bull.* 1984, **11**, 401
26 Leising, G. *Polymer* 1984, **25** (*Commun.*), 201
27 Chien, J. C. W., Karasz, F. E. and Shimamura, K. *Macromolecules* 1982, **15**, 1012
28 Baughman, R. H., Hsu, S. L., Pez, G. P. and Signorelli, A. T., *J. Polym. Sci. Polym. Lett. Edn.* 1979, **17**, 185
29 Chien, J. C. W. 'Polyacetylene—Chemistry, Physics and Material Science', Academic Press (1984)
30 Leiser, G., Wegner, G., Weizenhofer, R. and Brombacher, L. *Polym. Prepr.* 1984, **25**, 100
31 Leising, G., Leitner, P. and Kahlert, H. *Mol. Cryst. Liq. Cryst.* 1985, **117**, 67
32 Gibson, H. W., Weagley, R. J., Prest, W. M., Mosher, R. and Kaplan, S. *J. de Physique* 1983, **44**(C3), 123
33 Akaishi, T., Miyasala, K., Ishiawa, K., Shirakawa, H. and Ikeda, S. *J. Polym. Sci. Polym. Phys. Edn.* 1980, **18**, 745
34 Meyer, W. H. *Mol. Cryst. Liq. Cryst.* 1981, **77**, 137
35 Bunn, C. W. *Trans. Faraday Soc.* 1939, **35**, 428
36 Baughman, R. H., Hsu, S. L., Anderson, L. R., Pez, G. P. and Signorelli, A. J. in 'Molecular Metals', Plenum, N.Y., 189 (1978)
37 Chien, J. C. W. and Karasz, F. E. *Makromol. Chem., Rapid Commun.* 1982, **3**, 655.
38 Yanonni, C. S. and Clark, T. C. *Phys. Rev. Lett.* 1983, **51**, 1191
39 Moon, Y. B., Winokur, M., Heeger, A. J., Barker, J. and Bott, D. C. To be published
40 Wind, R. A., Duijvestijn, M. J. and Vriend, J. *Solid State Commun.* 1985, **56**, 713
41 Friend, R. H., Bradley, D. D. C., Pereira, C. M., Townsend, P. D., Bott, D. C. and Williams, K. P. J. *Synth. Met.* 1985, **13**, 101
42 Kuzmany, H., Imhoff, E. A., Fitchen, D. B. and Sarhangi, A. *Phys. Rev. B* 1982, **26**, 7109
43 Brivio, G. P. and Mulazzi, E. *Phys. Rev. B* 1984, **30**, 876
44 Stamm, M., Hocker, J. and Axmann, A. *Mol. Cryst. Liq. Cryst.* 1981, **77**, 125
45 Pouget, J. P., in 'Electronic Properties of Polymers and Related Compounds (Solid State Sciences 63)', Springer, Berlin p. 26 (1985)
46 Thompson, A. H. *Physica* 1980, **99B**, 100
47 Thompson, A. H. *Phys. Rev. Lett.* 1978 **40**, 1511
48 Thompson, A. H. *J. Electrochem. Soc.* 1979, **126**, 608
49 Thompson, A. H. *Rev. Sci. Instrum.* 1983, **54**(2), 229
50 Raleigh, D. O. and Crowe, H. R. *J. Electrochem. Soc.* 1969, **116**, 40
51 Shacklette, L. W., Toth, J. E., Murthy, N. S. and Baughman, R. H. *J. Electrochem. Soc.* 1985, **132**, 1529
52 Mott, N. F. and Davis, E. A. in 'Electronic Processes in Noncrystalline Materials', Clarendon Press, Oxford 1979, p. 209
53 Chen, J., Chung, T.-C., Moraes, F. and Heeger, A. J. *Solid State Commun.* 1985, **53**, 757
54 Moraes, F., Chen, J., Chung, T.-C. and Heeger, A. J. *Synth. Met.* 1985, **11**, 271
55 Shacklette, L. W., Murthy, N. S. and Baughman, R. H. *Mol. Cryst. Liq. Cryst.* 1985, **121**, 201
56 Baughman, R. H., Shacklette, L. W., Murthy, N. S., Miller, G. G. and Elsenbaumer, R. L. *Mol. Cryst. Liq. Cryst.* 1985, **118**, 253
57 Baughman, R. H., Murthy, N. S. and Miller, J. J. *J. Chem. Phys.* 1983, **79**, 515